Kovove Mater. 61 2023 199–204
DOI: 10.31577/km.2023.3.199

Microhardness and corrosion behavior of thermally treated $Fe_{38}Ni_{36}B_{18}Si_8$ metallic glass

Maja Đekić, Jelena Ostojić, Hađer Sinanović, Fehim Korać, Amra Salčinović Fetić*

Faculty of Science, University of Sarajevo, Zmaja od Bosne 33-35, 71 000 Sarajevo, Bosnia and Herzegovina

Received 16 May 2022, received in revised form 10 February 2023, accepted 10 March 2023

Abstract

This study aimed to investigate the influence of temperature and time of thermal treatment on the microhardness and corrosion behavior of Fe-Ni-based metallic glass. The investigation was carried out on metallic glass with a composition of $Fe_{38}Ni_{36}B_{18}Si_8$. The samples were isothermally treated in an ambience atmosphere for different time intervals. The microstructure examination revealed that (Fe,Ni), Fe_3Si, and $Ni_{31}Si_{12}$ phases were present in the amorphous matrix after the thermal treatment. The results showed that microhardness increases with the increase of annealing temperature. However, even a short exposure of the as-cast sample to a high temperature significantly improves its microhardness. Corrosion behavior investigation showed that the amorphous sample in both NaCl and HCl media has the lowest tendency to corrosion.

K e y w o r d s: metallic glass, thermal treatment, microhardness, corrosion properties

1. Introduction

Fe-based metallic glasses have been in the focus of scientific interest because of their good microhardness properties, strong corrosion resistance, and soft ferromagnetic properties [1–3]. This makes Fe-based metallic glasses good candidates for different applications in electronics, such as magnetic sensors, inductor cores, linear actuators, and corrosion-resistant coatings [1]. Their attractive properties can further be tailored for technological use by the controlled addition of Ni, which can improve their corrosion resistance while retaining their soft magnetic properties [4]. It is well known that the thermal treatment of metallic glasses leads to their structural relaxation, which consequently changes their physical properties [5]. Annealing below the glass transition temperature (T_g) can reduce residual stress [6, 7] and improve mechanical and soft magnetic properties in these materials [8, 9]. A number of authors investigated the influence of structural changes on the mechanical properties of metallic glasses [10, 11]. Namely, following thermal treatment in an inert atmosphere, according to [12], Fe-based metallic glasses with nanocrystals embedded in an amorphous matrix exhibited soft magnetic and mechanical properties superior to their amorphous and crystalline counterparts. In general, corrosion is a destruction of a certain material, and therefore classified as a harmful phenomenon. Metallic glasses have many good mechanical properties, which makes them desirable for a wide field of applications, but the tendency to corrosion greatly limits their practical use. In certain corrosive conditions, the corrosion resistance of some Co-, Ni-, and Fe-based bulk metallic glasses has been found to be better than that of the routinely used corrosion-resistant stainless steel (SUS 316L) [13]. It has been shown that by embedding protective components into the passive film or slowing the decomposition rate of the overlying metallic substrate, the addition of particular elements might improve corrosion resistance [14]. So far, there are few data reports on metallic glass corrosion behavior and the electrochemical mechanisms behind it. Metallic glass corrosion behavior is complex because it depends on chemistry, the structure of metallic glass, and finally, it depends on surface states in a variety of conditions. Corrosion can be determined in an acidic or basic environment, depending on the planned application of a certain metallic glass. In this paper, we investigate the effect of thermal treatment both on mechanical

*Corresponding author: amra.s@pmf.unsa.ba

Table 1. The names of the samples, annealing temperatures T_A and times of isothermal treatment t

Sample	T_A (K)	t (min)
FN0	as-cast	0
FN1	673	1
FN2	673	5
FN3	673	10
FN4	673	15
FN5	673	20
FN6	873	5
FN7	723	5

properties, specifically microhardness, and on corrosion properties of $Fe_{38}Ni_{36}B_{18}Si_8$ metallic glass.

2. Experimental

The samples of $Fe_{38}Ni_{36}B_{18}Si_8$ metallic glass ribbons were produced by a home-made melt-spinner and characterized by standard characterization techniques, such as scanning electron microscopy (SEM), X-ray diffraction (XRD), scanning differential calorimetry (DSC), and transport measurements, as described in [15].

A series of annealed samples were prepared in an ambience atmosphere in the furnace Nabertherm with a program controller S19. The samples, designated as FN1, FN2, FN3, FN4, and FN5, were maintained in isothermal conditions at 673 K for different time intervals (1, 5, 10, 15, and 20 min). According to the results of the previous DSC analysis [15], the temperature of 673 K is some 10 K lower than the glass transition temperature T_g. The sample designated as FN6 was isothermally treated for 5 min at 873 K, which is the temperature of its almost complete crystallization. The sample FN7 was heated for 5 min at 723 K, which is the temperature of the onset of crystallization. All the samples, together with the conditions of their isothermal treatment, are presented in Table 1.

X-ray diffraction (XRD) spectra were acquired on XPERT-PRO powder diffractometer (PANalytical) equipped with Cu source at 40 kV and 40 mA, multilayer parabolic mirror, and PIXcel^{1D} detector with Ni filter. Data were collected with 0.026 diffraction angle, and the collection time was 132.6 s/step. The samples were examined on the rotating monocrystalline Si holder.

Microhardness measurements on all the samples were performed with a DHV-1000Z Micro Vickers Hardness Tester device equipped with a pyramidal indenter with a 136° angle square base.

The loading time was 15 s, and the load was 0.981 N, with up to 10 measurements on each individual sample. The results of microhardness measurements are given as the average values of the individual measurements.

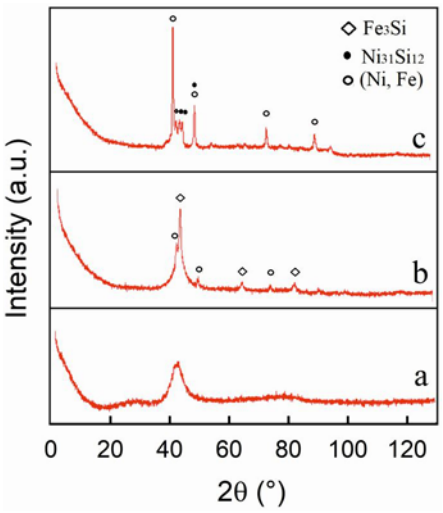

Fig. 1. XRD spectra of $Fe_{38}Ni_{36}B_{18}Si_8$ metallic glass ribbon: (a) FN0-as-cast, (b) FN2-thermally treated at 673 K for 5 min, and (c) FN6-thermally treated at 873 K for 5 min.

Corrosion behavior was tested in two different media, 0.5M NaCl and 0.5M HCl, by electrochemical measurements at room temperature, using Princeton Applied Research 263A potentiostat and a three-electrode cell. A platinum electrode was used as the counter electrode and Ag/AgCl as the reference electrode. Electrochemical/potentiodynamic polarization curves were measured with a potential scan rate of 0.167 mV s^{-1}. The scan rate used is chosen because the ASTM method recommends a scan rate of 0.1667 mV s^{-1}, yet the faster scan rates often result in distorted data because the sample cannot remain relatively stable. Prior to electrochemical measurements, the samples were degreased in acetone, washed thoroughly in distilled water, and air-dried. Electrochemical measurements were carried out on raw and annealed samples.

3. Results and discussion

3.1. Structure

XRD spectra of the as-cast sample FN0 and samples FN2 and FN6, which were thermally treated for 5 min at different temperatures in the ambient atmosphere, are presented in Figs. 1a,b,c. The raw sample (Fig. 1a) shows a relatively broad peak at around 45° which clearly indicates its amorphous structure. XRD spectra of the thermally treated samples show a series of structural transformations.

Table 2. XRD data for sample FN2

Position $2\theta(^\circ)$	Relative intensity (%)	Phase
44.02	54	(Ni,Fe)
45.28	100	Fe_3Si
51.36	12	(Ni,Fe)
66.02	10	Fe_3Si
75.45	6	(Ni,Fe)
83.61	11	Fe_3Si

Table 3. XRD data for sample FN6

Position 2θ (°)	Relative intensity (%)	Phase
41.57	3	$Ni_{31}Si_{12}$
42.90	3	$Ni_{31}Si_{12}$
43.68	100	(Fe,Ni)
44.61	22	Fe_3Si
45.95	19	$Ni_{31}Si_{12}$
46.82	22	$Ni_{31}Si_{12}$
50.88	31	(Fe,Ni); $Ni_{31}Si_{12}$
56.58	3	$Ni_{31}Si_{12}$
65.10	3	Fe_3Si
67.84	3	$Ni_{31}Si_{12}$
74.89	13	(Fe,Ni)
79.60	3	$Ni_{31}Si_{12}$
82.39	2	Fe_3Si
90.96	14	(Fe,Ni)
96.47	6	(Fe,Ni)

Figure 1b represents XRD data for the FN2 sample, where sharp peaks indicate crystalline phases that start to emerge in the amorphous matrix after annealing. The crystalline phases are identified as: (Fe,Ni) and Fe_3Si, and their positions and relative intensities are given in Table 2.

Besides the previously mentioned phases, XRD data for the FN6 sample (Fig. 1c) show the appearance of a new crystalline phase $Ni_{31}Si_{12}$ (Table 3).

3.2. Microhardness

The results of microhardness measurements are shown in Fig. 2. The average microhardness of the raw sample is determined to be (6.5 ± 0.3) GPa. According to our XRD results, the first signs of crystallization start to appear at 673 K. Even a very short annealing time of just 1 min at this temperature, increases the microhardness value by about 1.2 GPa. Furthermore, there is a clear increase in microhardness for all thermally treated samples at 673 K as compared to the as-cast sample, regardless of the time of treatment. No significant differences in microhardness were noticed

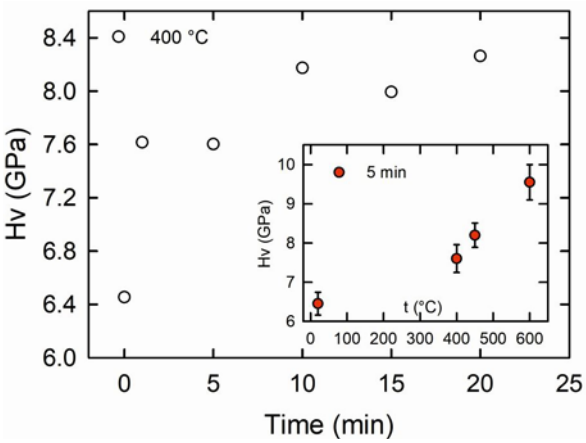

Fig. 2. Mean values of microhardness measurements for the raw sample and thermally treated samples for different time intervals together with measurement errors.

for different times of thermal treatment at this temperature. A similar result was observed in [20], where the authors noticed that different times of thermal treatment had no significant impact on the microhardness values. On the other hand, the additional thermal treatment of Fe-Ni amorphous alloy at higher temperatures significantly increases microhardness (inset of Fig. 2). The sample FN7, which was isothermally treated at 723 K for 5 min, shows improvement of its microhardness properties as compared to its amorphous counterpart. Annealing at 873 K leads to almost complete crystallization of the remainder of the amorphous phase and further increases microhardness. In summary, our results indicate that annealed samples have better microhardness properties than the as-cast sample, and microhardness increases with the increase of the annealing temperature. Also, even a very short isothermal treatment (1 or 5 min) in an ambient atmosphere can improve microhardness. Different authors [16, 17] observed the increase in microhardness with the increase in annealing temperature in metallic glasses. Zha et al. [16] attribute this hardening to the increase in the amount and fraction of crystalline phases in the amorphous matrix.

3.3. Corrosion

As it is known, corrosion in aqueous media is an electrochemical process due to the electrical conduction properties of two phases, electron conduction in the metallic phase and ionic conduction in the aqueous phase. The electrochemical reaction allows charge transfer at the interface between the metal (electrode) and the electrolyte. The electrochemical corrosion mechanism includes two reactions, anodic (oxidation) and cathodic (reduction).

In the anodic reaction, a metal M is oxidized:

$$M \rightarrow M^{n+} + ne^{-}, \quad (1)$$

or it can be said that an anodic reaction is actually the decomposition of metal.

Occurring at the same time and at the same rate, the reduction process provides the gain of electrons. The cathodic reaction generally consists of the reduction of dissolved oxygen when oxygen is present in the atmosphere and in solutions exposed to the atmosphere. The cathodic reaction is dependent on the corrosion media, and the supposed reactions should be as follows:

$$O_2 + 4H^+ + 4e \rightarrow 2H_2O \text{ (in acid solution)}, \quad (2)$$

$$2H_2O + O_2 + 4e \rightarrow 4OH^- \text{ (in neutral and alkaline solutions)}. \quad (3)$$

Environmental conditions influence the corrosion behavior of Fe-based metallic glasses. Intuitively, if the solution's abrasiveness is stronger, the corrosion resistance of metallic glass will be lower. It is generally agreed that if the corrosion potential is higher, it will be more difficult for oxidation reactions to occur in metals. Moreover, the larger the corrosion current density, the higher the corrosion rate. The corrosion resistance of metallic glasses is also influenced by the addition of metalloids such as B, Si, P, S, Ni, and C [18].

Electrochemical techniques are common techniques used to study the corrosion behavior of metallic glasses in different corrosion media. The widespread electrochemical technique engaged in measuring the corrosion behavior of metals or other materials such as alloys, or in this case, metallic glasses, is potentiodynamic polarization (Tafel analysis). The method is fast, and easy to perform.

In this study, we investigated the corrosion behavior of the as-cast sample (FN0) and of the samples annealed for 5 min at two different temperatures (FN2 and FN6).

Regarding general corrosion presented in Fig. 3, active dissolution in NaCl electrolyte started at a lower corrosion potential, than in HCl electrolyte. With the increase of pH value, it is attained that more negative corrosion potential is obtained, and the corrosion current density is decreased.

The corrosion potential becomes increasingly negative when the acidic ion or hydroxyl ion concentration rises, whereas the corrosion current density rises in general. That is, as acidic and hydroxyl ion content rise, corrosion resistance diminishes.

Important corrosion parameters, such as the corrosion potential (E_{corr}) and corrosion current (I_{corr}) of the tested samples, are summarized in Tables 4 and 5 in NaCl and HCl media, respectively.

In NaCl solution, the as-cast sample FN0 has the lowest corrosion current, followed by the sample annealed at 873 K (FN6). The highest corrosion current is found to be for the sample treated at 673 K (FN2).

The sample annealed at 873 K, as demonstrated earlier in Table 3, showed the appearance of a new crystalline phase $Ni_{31}Si_{12}$. This crystalline phase is already proven to have a low corrosion tendency [4].

In the HCl solution, the corrosion current is the lowest for the raw sample, followed by the current for the sample annealed at 673 K. The highest corrosion current is in the case of the sample annealed at 873 K. This means that in both media, the amorphous sample has the lowest tendency to corrosion which is in accordance with previously reported papers [4, 19].

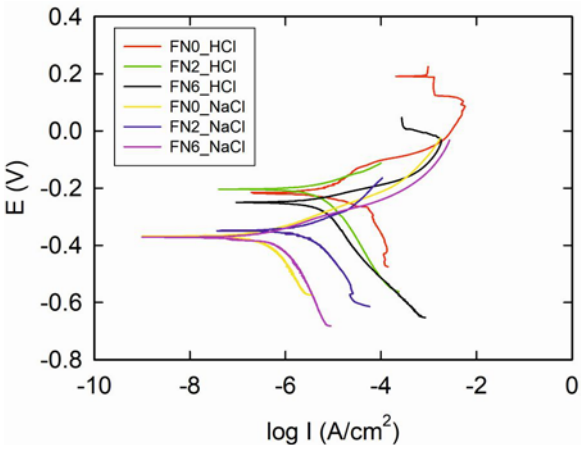

Fig. 3. Electrochemical polarization curves of FeBNiSi metallic glasses in the 0.5 M HCl and 0.5 M NaCl solution: (a) raw FN0, (b) annealed at 673 K FN2, and (c) annealed at 873 K FN6.

Table 4. Values of corrosion parameters of potentiodynamic polarization for raw and annealed samples in 0.5M NaCl

Sample	E_{corr} (mV)	I_{corr} (μA)
FN0	–367.5	0.319
FN2	–346.38	1.950
FN6	–371.97	0.443

Table 5. Values of corrosion parameters of potentiodynamic polarization for raw and annealed samples in 0.5M HCl

Sample	E_{corr} (mV)	I_{corr} (μA)
FN0	–220.7	2.529
FN2	–202.4	3.665
FN6	–249.9	5.986

The authors attribute this to the homogeneous state of the amorphous sample, which does not contain dislocations, nor grain boundaries, or any other defects.

Corrosion is usually caused by a loose-packing structure and the existence of flaws from a structural standpoint. Thus, the loose atomic packing allows for a free area for chloride ions penetration [20].

Moreover, the faster migration of silicon ions to the surface in the crystalline structure promotes SiO_2 film formation, which enhances the corrosion properties [21].

Because metallic glasses are metastable and can be converted to a stable crystalline phase through heat treatment or mechanical manipulation, structural changes might also affect corrosion resistance.

4. Conclusions

In this paper, we examined the influence of thermal treatment in an ambience atmosphere on the microhardness and corrosion properties of $Fe_{38}Ni_{36}B_{18}Si_8$ metallic glass. Our results show that microhardness improves with the increase in the annealing temperature. Also, even a very short time of thermal treatment, namely 1 min, significantly improves microhardness. There is no significant difference in microhardness value when the time of treatment is extended. Regarding the corrosion resistance, our results are in an agreement with previous research from this field, confirming that amorphous alloys display higher corrosion resistance. This means that it is necessary to find a compromise between the microhardness and corrosion resistance of a specific sample in accordance with a particular application. According to our results, samples with crystalline phases are not suitable for usage in a corrosive environment.

Acknowledgements

We would like to thank the late Redžep Baltić for the production of the Fe-based metallic glass. This study was supported by the project Investigation of the influence of heat treatment on the microhardness of some metallic glasses financed by the Ministry of Science, Higher Education and Youth, Canton Sarajevo, Federation of Bosnia and Herzegovina, Bosnia and Herzegovina (Grant no. 2702114125028, the year 2021).

References

[1] H. X. Li, Z. C. Lu, S. L. Wang, Y. Wu, Z. P. Lu, Fe-based bulk metallic glasses: Glass formation, fabrication, properties and applications, Prog. Mater. Sci. 103 (2019) 235–318. https://doi.org/10.1016/j.pmatsci.2019.01.003

[2] C. R. M. Afonso, C. Bolfarini, W. J. Botta Filho, C. S. Kiminami, In-situ crystallization of amorphous $Fe_{73-x}Nb_xAl_4Si_3B_{20}$ alloys through synchrotron radiation, J. Non-Cryst. Solids 352 (2006) 3404–3409. https://doi.org/10.1016/j.jnoncrysol.2006.03.078

[3] J. W. Li, A. N. He, B. L. Shen, Effect of Tb addition on the thermal stability, glass-forming ability and magnetic properties of Fe-B-Si-Nb bulk metallic glass, J. Alloys Compd. 586 (2014) 546–549. https://doi.org/10.1016/j.jallcom.2012.09.087

[4] M. M. Vasić, T. Žák, N. Pizúrová, I. Stojković Simatović, D. M. Minić, Influence of thermal treatment on microstructure and corrosion behavior of amorphous $Fe_{40}Ni_{40}B_{12}Si_8$ alloy, Metall. Mater. Trans. A 52 (2021) 34–45. https://doi.org/10.1007/s11661-020-06079-3

[5] L. Song, W. Xu, J. Huo, J.-Q. Wang, X. Wang, R. Li, Two-step relaxation in metallic glasses during isothermal annealing, Intermetallics 93 (2018) 101–105. https://doi.org/10.1016/j.intermet.2017.11.016

[6] Z. Lu, W. Jiao, W. H. Wang, H. Y. Bai, Flow unit perspective on room temperature homogeneous plastic deformation in metallic glasses, Phys. Rev. Lett. 113 (2014) 045501. https://doi.org/10.1103/physrevlett.113.045501

[7] M. Aljerf, K. Georgarakis, A. R. Yavari, Shaping of metallic glasses by stress-annealing without thermal embrittlement, Acta Mater. 59 (2011) 3817–3824. https://doi.org/10.1016/j.actamat.2011.02.039

[8] H. B. Yu, X. Shen, Z. Wang, L. Gu, W. H. Wang, H. Y. Bai, Tensile plasticity in metallic glasses with pronounced β relaxations, Phys. Rev. Lett. 108 (2012) 015504. https://doi.org/10.1103/PhysRevLett.108.015504

[9] A. Wang, C. Zhao, H. Men, A. He, C. Chang, X. Wang, R.-W. Li, Fe-based amorphous alloys for wide ribbon production with high B_s and outstanding amorphous forming ability, J. Alloys Compd. 630 (2015) 209–213. https://doi.org/10.1016/j.jallcom.2015.01.056

[10] D. M. Minić, A. Gavrilović, P. Angerer, D. G. Minić, A. Maričić, Structural transformations of $Fe_{75}Ni_2Si_8B_{13}C_2$ amorphous alloy induced by thermal treatment, J. Alloys Compd. 476 (2009) 705–709. https://doi.org/10.1016/j.jallcom.2008.09.072

[11] A. Hitit, Effect of annealing on microstructure and microhardness of Co-Fe-Ni-Ta-B-Si bulk metallic glass, J. Mater. Sci. Technol. 31 (2015) 148–152. https://doi.org/10.1016/j.jmst.2014.09.004

[12] D. M. Minić, Influence of thermally induced structural transformations on hardness in $Fe_{89.8}Ni_{1.5}Si_{5.2}B_3C_{0.5}$ amorphous alloy, J. Alloys Compd. 509 (2011) 8350–8355. https://doi.org/10.1016/j.jallcom.2011.03.011

[13] A. Inoue, X. M. Wang, W. Zhang, Development and application of bulk metallic glasses, Rev. Adv. Mater. Sci. 18 (2008) 1–9.

[14] K. Weller, Thermodynamics and kinetics of the oxidation of amorphous Al-Zr alloys. Max-Planck-Inst. Intell. Syst. 2015.

[15] K. Hrvat, M. Lozančić, S. Sulejmanović, I. Gazdić, N. Bajrović, A. Salčinović Fetić, Investigation of partially crystalline metallic glass $Fe_{38}Ni_{36}B_{18}Si_8$, IOP: Conference Series 1814 (2021) 012003. https://doi.org/10.1088/1742-6596/1814/1/012003

[16] G. Zha, Effects of annealing temperature on microstructure and hardness of $(Cu_{60}Zr_{30}Ti_{10})_{98}Y_2$ bulk metallic glass, J. Rare Earths 28 (2010) 243–245. https://doi.org/10.1016/j.msea.2005.07.020
[17] Z. Zhang, Influence of relaxation and crystallization on micro-hardness and deformation of bulk metallic glass, Mater. Sci. Eng. A 407 (2005) 161–166. https://doi.org/10.1016/S1002-0721(09)60088-0
[18] S. J. Pang, T. Zhang, K. Asami, A. Inoue, Bulk glassy Fe-Cr-Mo-C-B alloys with high corrosion resistance, Corros. Sci. 44 (2002) 1847–1856. https://doi.org/10.1016/S0010-938X(02)00002-1
[19] S. Wang, Corrosion Resistance and Electrocatalytic Properties of Metallic Glasses. In: B. Movahedi (Ed.), Metallic Glasses – Formation and Properties, IntechOpen, London 2016. https://doi.org/10.5772/63677
[20] D. Liang, J.-C. Tseng, X. Liu, Y. Cai, G. Xu, J. Shen, Investigation of the structural heterogeneity and corrosion performance of the annealed Fe-based metallic glasses, Materials 14 (2021) 929. https://doi.org/10.3390/ma14040929
[21] C. A. C. Souza, S. E. Kuri, F. S. Politti, J. E. May, C. S. Kiminami, Corrosion resistance of amorphous and polycrystalline FeCuNbSiB alloys in sulphuric acid solution, J. Non-Cryst. Solids 247 (1999) 69–73. https://doi.org/10.1016/S0022-3093(99)00034-4